Valence-band photoemission study of single crystalline CeNiSn

J.-S. Kang
Department of Physics, The Catholic University of Korea, Puchon 422-743, Korea

C. G. Olson
Ames Laboratory, Iowa State University, Ames, Iowa 50011

Y. Inada and Y. Ōnuki
Graduate School of Science, Osaka University, Toyonaka 560, Japan

S. K. Kwon and B. I. Min
Department of Physics, Pohang University of Science and Technology, Pohang 790-784, Korea
(Received 10 November 1997; revised manuscript received 27 March 1998)

The electronic structure of single crystalline CeNiSn has been investigated using photoemission spectroscopy. The extracted Ce $4f$ spectrum exhibits three peak structures; the typical Fermi level and 2 eV peaks, and another between them, $\sim$0.9 eV below the Fermi level E_F. The near-E_F peak reflects a substantial Ce $4f$-Sn sp hybridization, whereas the 0.9 eV peak arises from the Ce $4f$-Ni $3d$ and Ce $5d$-Ni $3d$ hybridization. A Ni $3d$ satellite feature is observed about 6 eV below the Ni $3d$ main band, indicating a strong Ni $3d$ Coulomb correlation in CeNiSn. The high-resolution photoemission study indicates a finite metallic density of states at E_F, implying a semimetallic ground state. The electronic states near E_F are found to have mixed character from the Sn sp, Ce $5d$, Ce $4f$, and Ni $3d$ electrons. Constant-initial-state and constant-final-state yield spectra across the $4d \rightarrow 4f$ threshold indicate the Ce valence to be close to 3+. [S0163-1829(98)04131-9]

I. INTRODUCTION

CeNiSn has attracted much attention because of its very small pseudogap of a few K.[1–3] CeNiSn crystallizes in the orthorhombic $\epsilon-$TiNiSi structure belonging to the noncentrosymmetric space group $Pn2_1a$, which causes a strong anisotropy in magnetic and electronic properties.[2,4,5] Early transport and magnetic measurements on CeNiSn indicated the energy gap formation in the nonmagnetic ground state below $T_g \approx 6$ K (T_g: the gap formation temperature), with the estimated Kondo temperature T_K of 40–80 K.[6] Recent experiment on the temperature (T) dependence of the electrical resistivity in a purified single crystal of CeNiSn (Refs. 5 and 7) indicated a metalliclike ground state. Therefore the semiconductorlike T-dependent electrical resistivity observed in early samples is considered to be presumably due to carrier localization by impurities. In contrast, inelastic neutron scattering experiments on single crystal samples[8,9] showed the existence of anisotropic pseudogap-type magnetic excitations. The specific heat of single-crystal CeNiSn also shows a sharp decrease at low temperature after reaching a maximum around 7 K,[10] which is regarded as evidence for the development of the pseudogap. A V-shaped density of states (DOS) near the Fermi level E_F was inferred from the nuclear magnetic resonance relaxation rate[11] and thermodynamic properties.[12]

CeNiSn thus seems to exhibit an apparent contradiction between the metallic conductivity and the gapwise behavior of the thermodynamic properties and the spin response. To resolve such a contradiction and to get information about the origin of the pseudogap formation in CeNiSn, it is important to investigate its electronic structure. Band-structure calculations predict CeNiSn to be either a semimetal,[13] with a pseudogap that closes along some directions, or a small-gap insulator with an anisotropic hybridization gap and a V-shaped DOS near E_F.[14] Some models based on a spin gap[15] or a hybridization-induced charge gap[16] have been proposed to explain the pseudogap formation. In the former model, the ground state is assumed to be the Kondo spin singlet and the spin gap corresponds to the energy difference between the spin singlet and triplets. In the latter model, it is argued that an anisotropic hybridization gap reflects the $\vec{\mathbf{k}}$-dependent hybridization matrix elements and that the shape of the DOS around E_F is significantly deformed with impurity concentration. Kagan *et al.*[6] developed the spin fermion theory, including the crystal-field levels, and found a fairly good explanation for experiments such as neutron scattering and specific heat. Only a few experimental studies have been reported on the electronic structure of CeNiSn.[17,18] Based on valence-band and core-level photoemission spectroscopy (PES) measurements,[17] it has been argued that Ce is close to trivalent and that the Ce $4f$ electrons are strongly hybridized with the Sn sp electrons. Unfortunately, these experiments were done on polycrystalline samples. In view of the recent reports of metalliclike behavior, it is important to carry out experiments on high-quality single-crystal samples.

Neither the predicted anisotropic electronic structure nor the valence of Ce has been confirmed. Angle-resolved photoemission spectroscopy (ARPES) measurements of CeNiSn along different symmetry directions allow the examination of the anisotropic electronic structure. Resonant photoemission provides a method to separate emissions from different valence states[19] because the intermediate state of the $4d \rightarrow 4f$ resonance is dependent upon the f occupancy, yielding dif-

ferent photon energy dependences in the constant-initial-state (CIS) spectra. Constant-final-state (CFS) spectra for the mixed valent material will show absorption features due to two different valence states.[20]

In this paper we report a resonant photoemission study of high-quality single crystalline CeNiSn near the Ce $4d \rightarrow 4f$ absorption edge, together with CIS and CFS yield measurements. Both the partial spectral weight (PSW) distribution of Ce $4f$ electrons and the bulk Ce valence have been determined. In addition, high-resolution photoemission measurements have been performed at low photon energies, which allows us to determine the character of electronic states near E_F.

II. EXPERIMENTAL DETAILS

Single crystals of CeNiSn were grown by the Czochralski pulling method by using a tungsten crucible in an rf furnace under purified helium gas at a pressure of 4 kg/cm^2. Ingots were 4–5 mm in diameter and 50 mm in length. The ingots were determined to be single crystal from x-ray Laue patterns. Photoemission experiments were carried out at the Ames/Montana ERG/Seya beam line at the Synchrotron Radiation Center. The samples were cleaved in vacuum with a base pressure better than 4×10^{-11} Torr. Samples were cooled down to $T_{msr}\approx 20$ K using a closed cycle He refrigerator. The Fermi level and the overall instrumental resolution of the system were determined from the valence-band spectrum of a sputtered Pt foil. The total instrumental resolution [full width at half maximum (FWHM)], due to both the monochromator and the electron energy analyzer, was about 150 and 250 meV at $h\nu\sim 20$ and 120 eV, respectively. High-resolution photoemission spectra were taken with FWHM of 40–50 meV. The photon flux was monitored by the yield from a gold mesh and all the spectra reported are normalized to the mesh current.

III. RESULTS AND DISCUSSION

A. Energy distribution curves over wide $h\nu$ range

Figure 1 shows the valence band energy distribution curves (EDC's) of CeNiSn in the photon energy ($h\nu$) range of 14–121 eV, which includes both the Ni $3p$ and Ce $4d$ absorption thresholds. In our study, no angle-resolved effects were observed, probably because of the rough surface topography after cleavage. So the spectra in this paper can be considered angle integrated. The variation in the line shape with varying $h\nu$ reflects the change in the relative photoionization cross sections of different electronic states.[21] $h\nu=121$ eV and $h\nu=115$ eV correspond to the on- and off-resonance energies due to the Ce $4d\rightarrow 4f$ absorption, respectively.[22] Therefore the emission enhanced at $h\nu=121$ eV [between E_F and about 3 eV in binding energy (BE)] can be identified with the Ce $4f$ emission. This finding implies a substantial contribution from Ce $4f$ states to the emission close to E_F, which will be discussed further in connection with the results shown in Fig. 3.

The off-resonance spectrum at $h\nu=115$ eV is dominated by the Ni $3d$ emission. The main features in the EDC hardly change from $h\nu\approx 115$ eV down to $h\nu=63$ eV, consistent with dominant Ni $3d$ emissions in this photon energy range.[21] The intensity at E_F relative to that of the Ni $3d$ main peak (1.4 eV in BE) in this photon energy range also indicates the presence of Ni $3d$ states near E_F. $h\nu=68$ and 63 eV correspond to the Ni $3p\rightarrow 3d$ on- and off-resonance energies, respectively. At $h\nu=68$ eV, the main peak around 1.4 eV in BE and the satellite peak around 6 eV below the main peak can be roughly assigned to the $3d^9c^{m-1}$ and $3d^8c^m$ final-state configurations (assuming the initial-state configuration as $3d^9c^m$), respectively, as in pure Ni metal (c: conduction or ligand electrons).[23] The satellite structure associated with the Ni $3d$ bands cannot be explained by one electron band theory, since it arises from the Ni $3d$ Coulomb correlation.

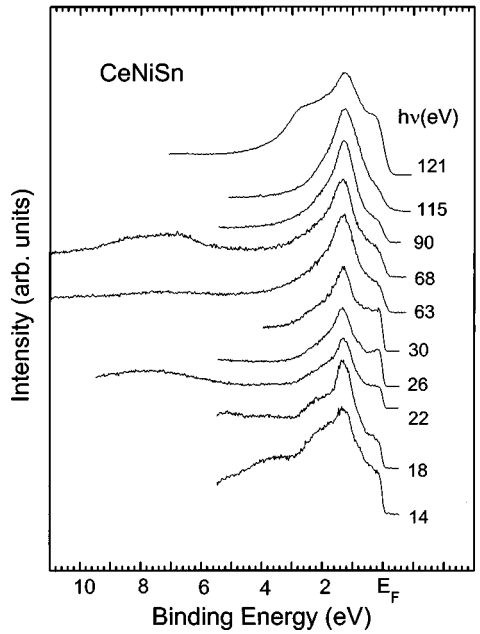

FIG. 1. EDC's of CeNiSn over a wide photon energy ($h\nu$) range.

At low $h\nu$'s (14–30 eV), besides the Ni $3d$ main peak at 1.4 eV BE, three other weak structures are observed; at E_F, $\sim$0.8 eV, and $\sim$2.2 eV in BE, which diminish with increasing $h\nu$. At these lower $h\nu$'s, the cross sections (σ) of Sn sp and Ce $5d$ states become comparable to that of the Ni $3d$ electrons,

$$\beta\equiv\frac{\sigma(Sn\ sp)+\sigma(Ce\ 5d)}{\sigma(Ni\ 3d)}\sim 2 \quad \text{at} \quad h\nu\sim 20\ \text{eV}, \tag{1}$$

whereas they become negligible at higher $h\nu$'s,

$$\beta<0.02 \quad \text{at} \quad h\nu\sim 80\ \text{eV}. \tag{2}$$

Therefore these three weak structures reflect the Sn sp and Ce $5d$ emissions. This conclusion implies that the Sn sp and Ce $5d$ states in CeNiSn are spread over the whole valence band, i.e., from E_F to $\sim$4 eV below.

In Fig. 1, a shoulderlike structure near E_F is observed, which has not been observed in Ref. 17. This difference reflects better energy resolution and the better quality of the samples employed in this study. This feature is more clearly seen in Fig. 2, which reveals the spectral trend near E_F with varying $h\nu$; As $h\nu$ decreases from 90 to 55 eV, the intensity

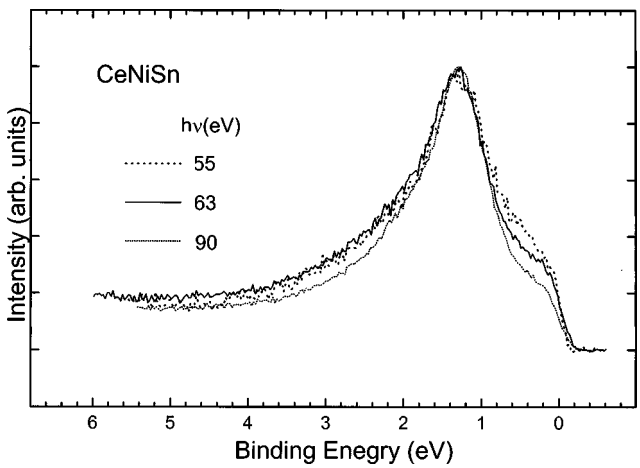

FIG. 2. Comparison of valence-band photoemission spectra of CeNiSn with $h\nu = 55,63,90$ eV.

at E_F increases slightly with respect to that of the Ni $3d$ main peak. This is due to the increase in the Sn sp and Ce $5d$ cross sections, with respect to that of the Ni $3d$ electrons: $\beta < 0.02$ at $h\nu \sim 90$ eV and $\beta < 0.1$ at $h\nu \sim 50$ eV. Thus the results shown in Fig. 2 confirm the presence of Sn sp and Ce $5d$ states near E_F. By combining the findings in Figs. 1 and 2, it is concluded that the electronic states at the Fermi edge in CeNiSn have mixed character, i.e., a mixture of the Sn sp, Ce $5d$, Ce $4f$, and Ni $3d$ character. Indeed this conclusion is consistent with our band-structure calculations,[24] in which the ground state of CeNiSn becomes semimetallic, and those states that cross E_F have dominant character of Ce $4f$ electrons (40–70 %) and also non-negligible contributions from the Ce $5d$ (5–25 %), Ni $3d$ (5–25 %), and Sn sp (8–10 %) electrons. These predictions are similar to those of Ref. 14, except that an the insulating ground state is predicted in Ref. 14.

B. Ce 4*f* spectrum

Figure 3 presents the subtraction procedure of the Ce $4d \rightarrow 4f$ off-resonance spectrum (dashed line) from the on-resonance spectrum (solid line), and the difference curve (dots) that is assumed to represent the extracted Ce $4f$ partial spectral weight (PSW) distribution. The off-resonance spectrum has been scaled to account for the $h\nu$ dependence of the Ni $3d$ cross section.[25] The difference curve exhibits three prominent features at about 0.3 eV (A), 0.9 eV (B), and 2.7 eV (C) in BE. In addition to the two peak structures (A,C), an extra peak B exists in the $4f$ derived PSW of CeNiSn. Any ambiguity in the extraction of the Ce $4f$ PSW and the nature of the structure B will be discussed further later in the context of the contribution from the Ce $5d$ PSW.

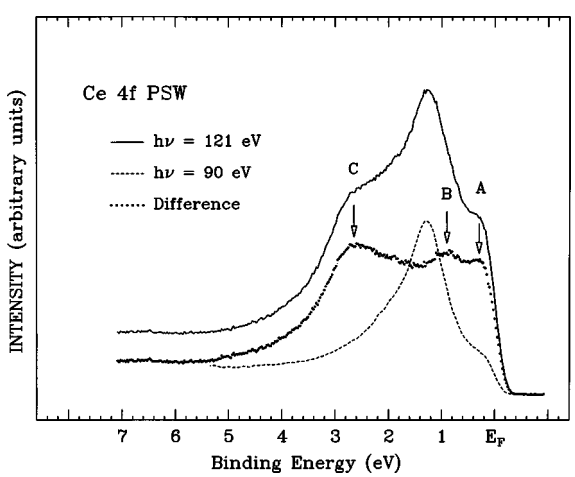

FIG. 3. The extracted Ce $4f$ spectrum (dots) of CeNiSn, obtained from subtraction of the Ce $4d \rightarrow 4f$ off-resonance spectrum (dashed lines) from the on-resonance spectrum (solid lines). See text for the details.

The peaks A and C are reminiscent of the well-known double-peak structures observed in Ce metal and Ce compounds. The peak C corresponds to the $4f^1 \rightarrow 4f^0$ transition,[26] while the $4f$ spectral intensity close to $E_F(A)$ is known to correspond to the $4f^1c^{m-1}$ final state and to reflect the strength of the hybridization between Ce $4f$ and conduction-band electrons in several different approaches.[22,27–29] In the LDA (local-density approximation) band theoretical view,[27] the peak near E_F is interpreted as the ground-state Ce $4f$ band, corresponding to the fully relaxed $4f^1c^{m-1}$ final states. However, the LDA band approach is not able to account for the strong Coulomb correlation in Ce $4f$ electrons. On the other hand, the Gunnarsson-Schönhammer (GS) theory[28] based on the degenerate impurity Anderson Hamiltonian (IAH), assuming Ce $4f$ electrons to be essentially localized, has been considered to be a good model for describing the Ce $4f$ electrons. According to the GS theory, the $4f$ spectral feature close to E_F corresponds to the tail of the Kondo resonance that originates from the hybridization interaction between Ce $4f$ and conduction-band electrons. In contrast, recent high-resolution PES studies on Ce compounds indicates that the T-dependence and/or $\vec{\mathbf{k}}$-dependent effects of Ce $4f$ near-E_F peaks are inconsistent with the predictions of the IAH model.[30–32] Therefore the detailed origin of the near E_F peak is still controversial.

Despite the controversy surrounding the origin of the near E_F feature, the high intensity of peak A suggests large hybridization, as explained below. The average separation between Ce sites in CeNiSn ($d = 3.82$ Å) (Ref. 4) is larger than the critical Ce-Ce distance in the Hill plot (3.3–3.5 Å),[33] beyond which the Ce $4f$ electrons are observed to form local moments. This separation is even larger than that in α-Ce (3.39 Å) and γ-Ce (3.65 Å),[27] suggesting that the direct interaction between near-neighbor Ce $4f$ electrons is negligible in CeNiSn. The interaction between Ce $4f$ electrons should be mediated by the hybridization between Ce $4f$ electrons and conduction-band electrons, such as Ce $5d$, Sn sp, and Ni $3d$ electrons. The Ni $3d$ wave function is more localized than the Ce $5d$ or Sn sp wave functions, yielding a smaller overlap with the $4f$ wave functions on nearest-neighbor Ce sites, and hence one expects the Ce $4f$–Ni $3d$ hybridization to be smaller than the Ce $4f$–Ce $5d$ or Ce $4f$–Sn sp hybridization. This argument is supported by the observation that the intensity of the main Ni $3d$ peak (at 1.4 eV in BE) is much stronger than that of the near E_F peak in the Ni $3d$ PSW, whereas, in the Ce $4f$ PSW, the intensity of peak A is comparable to that of peak B. In addition, the average nearest-neighbor separation between Ce and Sn atoms (3.27 Å) is much shorter than that between Ce and Ce

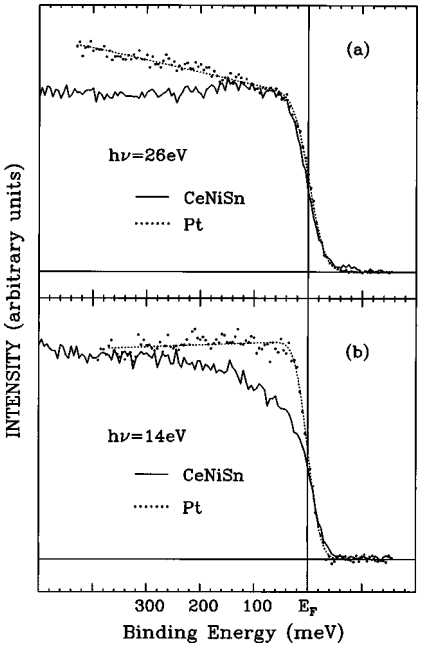

FIG. 4. High-resolution photoemission spectra of CeNiSn (solid lines) in the vicinity of the Fermi level taken at $h\nu = 14$ eV and 26 eV, in comparison with those of Pt metal (dots). All the spectra were obtained with the same measurement conditions; around 20 K and with the total resolution of 40–50 meV.

atoms (3.82 Å),[4] suggesting that the Ce $4f$–Sn sp hybridization is larger than the Ce $4f$–Ce $5d$ hybridization. Therefore we conjecture that the hybridization between Ce $4f$ and Sn sp electrons is the major origin of the near-E_F peak A in the Ce $4f$ PSW. To obtain a solid picture on the hybridization interaction in CeNiSn, it will be necessary to calculate hybridization matrix elements, which is in progress.

The Ce $5d$ emission is known to resonate at the $4d$ absorption edge as well.[34,35] Neither the portion nor the line shape of the Ce $5d$ PSW is known for CeNiSn yet, but it is likely that a substantial contribution from the Ce $5d$ PSW lies under the structure B, as explained below. It is interesting to note that the three peak structures of the Ce $4f$ PSW of CeNiSn (see the difference curve in Fig. 3) are also seen in $CeBe_{13}$.[34] In the case of $CeBe_{13}$, the Be sp PSW has two peaks, one near E_F and the other at about 1.5 eV in BE, with the latter being located near the middle peak in the Ce $4f$ PSW. The middle peak in $CeBe_{13}$ has been assigned mainly due to the Ce $5d$ PSW hybridized with the Be sp electrons. In CeNiSn, the peak B is located close to that of the Ni $3d$ main peak, suggesting that it is due to the hybridization to the Ni $3d$ electrons of the Ce $4f$ or $5d$ electrons. Moreover, since the Ce $5d$ wave functions have a larger overlap with the Ni $3d$ wave functions than the Ce $4f$ wave functions both in space and energy, it is likely that the feature B has a substantial contribution from the Ce $5d$ PSW.[36] This interpretation is consistent with the finding that no feature like B has been observed in the Ce $4f$ PSW of $CeSn_3$, in which the Sn sp PSW is rather structureless.[37]

C. High-resolution PES near the Fermi level

Figure 4 compares high resolution PES spectra of CeNiSn (solid lines) in the vicinity of E_F with those of Pt metal (dots). These spectra were taken with the same experimental conditions; at $T_{msr} \approx 20$ K, and with FWHM$=40-50$ meV. In this comparison, two spectra are scaled to each other. The dotted lines in the spectra of Pt metal are the results of a fitting using the Fermi-Dirac distribution function convoluted with a Gaussian function. In fitting the spectra of Pt, we have assumed a flat DOS with a nonzero slope that is cutoff at E_F by the Fermi-Dirac distribution function. The Gaussian function has been used to simulate the instrumental resolution.

The fact that the slope of the photoemission spectra of CeNiSn at E_F is very similar to that of Pt indicates a finite metallic DOS at E_F in CeNiSn. Even though the PES spectrum is measured above T_g, it should at least reflect the ground-state DOS. The finite metallic DOS would be consistent with the recent report of a metallic ground state[7] and a pseudogap that closes along some direction. The present analysis, however, does not eliminate the possible existence of a V-shaped DOS of width 5 meV at E_F (Ref. 12) because of the finite resolution. Further, there is a possibility of the V-shaped DOS that exists over only part of the Fermi surface. Our experiment does not allow to determine the anisotropic electronic structure of CeNiSn, because the spectra are effectively angle integrated.

Finally, it would be worthwhile to point out that, in our high-resolution photoemission measurements of CeNiSn, no spectral feature has been observed around 280 meV in BE that corresponds to the spin-orbit sideband of the Ce $4f^1$ final state.[38] This is probably because the PES spectrum at $h\nu = 26$ eV is not dominated by Ce $4f$ emission, but rather by Ni $3d$ and Sn sp emission.

D. Yield spectra and Ce valence

Figure 5 shows the yield spectra, taken in the CIS mode across the $4d \rightarrow 4f$ absorption threshold, for different initial state energies E_i in the valence band. The spectra have been scaled to have the same magnitude at the peak. Each CIS yield spectrum represents the $h\nu$ dependence of an initial state. The top curve is the CFS yield spectrum taken with a kinetic energy E_K of 2 eV. The well-known Fano-like resonance in the Ce $4f$ cross section is clearly observed in the CIS spectra in Fig. 5. The line shapes of the Ce $4f$ CIS and CFS yield spectra in CeNiSn are very similar to those of Ce metal,[39] for which the Ce valence is close to $3+$. Further, the line shape of the Ce $4f$ CIS in CeNiSn is essentially the same for different values of E_i over the Ce $4f$ PSW, indicating that the $4f$ emission does not have separate contributions from different valence states. Thus these Ce $4f$ CIS spectra provide evidence that the valence of Ce is close to $3+$ in CeNiSn. The CFS yield spectrum of CeNiSn shows no indication of a separate $4d \rightarrow 4f$ absorption process corresponding to a different valence state, also suggesting that strong mixed valence does not occur in CeNiSn. This conclusion will be confirmed by fine structures in the CFS spectrum (see Fig. 6 below). Drawing a quantitative conclusion on the valence of Ce, however, requires a detailed theoretical analysis of the $4f$ CIS.[40–42]

Figure 6 compares fine structures in the CFS yield spectrum of CeNiSn at the onset of the $4d$ absorption with those

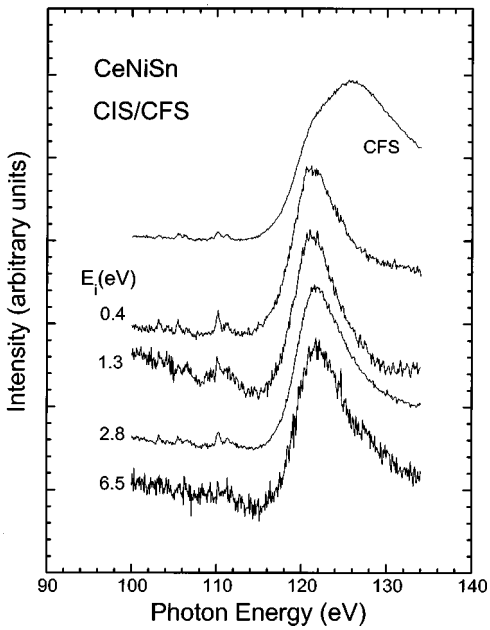

FIG. 5. CIS yield spectra of CeNiSn taken at initial state energies E_i of -0.4, -1.3, -2.8, and -6.5 eV, respectively. The spectrum at the top is the CFS yield spectrum taken with a kinetic energy E_K of 2 eV.

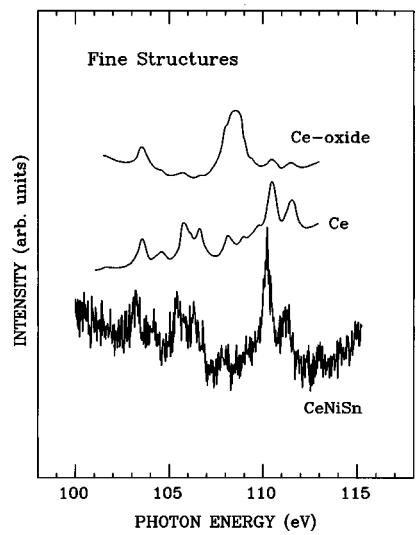

FIG. 6. Comparison of fine structures in the CFS yield spectra of CeNiSn to those in the absorption spectra of Ce metal and Ce oxide. The latter two spectra have been reproduced from Ref. 43.

in the absorption spectra of Ce metal and Ce oxide, which are reproduced from Haensel, Rabe, and Sonntag.[43] It is clearly shown that the CFS fine structures of CeNiSn are very similar to those in the absorption spectrum of Ce metal, but quite different from those of Ce oxide. It is known that the energy separations and relative strengths among the fine structures in the absorption spectrum of Ce oxide are very similar to those of La metal, but energy shifted from La due to the different core potential.[44] La metal has nearly no $4f$ electrons in the ground state, and hence this indicates that Ce ions in Ce oxide have nearly $4f^0$ configurations, which corresponds to the formal valence of Ce $4+$. Therefore the comparison in Fig. 6 provides a fingerprint that there is no formal Ce $4+$ state in CeNiSn, implying that the valence of Ce in CeNiSn is very close to $3+$.

IV. CONCLUSIONS

The electronic structure of single crystalline CeNiSn has been investigated using photoemission spectroscopy. The extracted Ce $4f$ PSW extends between E_F and about 3 eV below and exhibits three peak structures, including the well-known double peak structures and another peak located about $\sim$0.9 eV in BE. According to the $h\nu$ dependence of each feature, a large portion of the near-E_F peak arises from the Ce $4f$–Sn sp hybridization. The 0.9 eV peak reflects the Ce $4f$–Ni $3d$ hybridization, and it also has a non-negligible contribution from the Ce $5d$ PSW that arises from a large Ce $5d$–Ni $3d$ hybridization. At the Ni $3p \rightarrow 3d$ on-resonance energy, a satellite feature has been observed about 6 eV below the Ni $3d$ main band, indicating a strong Ni $3d$ Coulomb correlation in CeNiSn. The Sn sp and Ce $5d$ states are found to spread over the whole valence band, i.e., from E_F to $\sim$4 eV below.

The high-resolution photoemission study of CeNiSn indicates a finite DOS at E_F above T_g, suggesting a semimetallic ground state. The $h\nu$ dependence of the intensity at E_F indicates that the electronic states near E_F have mixed character of the Ce $4f$, Ce $5d$, Ni $3d$, and Sn sp electrons. CIS and CFS yield spectra near the $4d$ threshold are very similar to those of Ce metal, indicating that the Ce valence is close to $3+$.

ACKNOWLEDGMENTS

The authors acknowledge the financial support of the Korea Research Foundation (1997-001-D00139), and the Korea Science and Engineering Foundation (96-0702-01-01-3). The Ames Laboratory is operated by Iowa State University for the U.S. DOE (7405-ENG-82). One of us (Y.O.) was supported by a Grant-in-Aid for COE Research (10 CE 2004) of the Ministry of Education, Science, Sports and Culture in Japan. The Synchrotron Radiation Center is supported by NSF (DMR-95-31009).

[1] T. Takabatake, Y. Nakazawa, and M. Ishikawa, Jpn. J. Appl. Phys., Suppl. **26**, 547 (1987).

[2] T. Takabatake, M. Nagasawa, H. Fujii, G. Kido, M. Nohara, S. Nishigori, T. Suziki, T. Fujita, R. Helfrich, U. Ahlheim, K. Fraas, C. Geibel, and F. Steglich, Phys. Rev. B **45**, 5740 (1992).

[3] T. Ekino, T. Takabatake, H. Tanaka, and H. Fujii, Phys. Rev. Lett. **75**, 4262 (1995).

[4] I. Higashi, K. Kobayashi, T. Takabatake, and M. Kasaya, J. Alloys Compd. **193**, 300 (1993).

[5] Y. Inada, H. Azuma, R. Settai, D. Aoki, Y. Ōnuki, K. Kobayashi,

T. Takabatake, G. Nakamoto, H. Fujii, and K. Maezawa, J. Phys. Soc. Jpn. **65**, 1158 (1996).

[6] Y. Kagan, K. A. Kikoin, and A. S. Mishchenko, Phys. Rev. B **55**, 12 348 (1997).

[7] G. Nakamoto, T. Takabatake, H. Fujii, A. Minami, K. Maezawa, I. Oguro, and A. A. Menovsky, J. Phys. Soc. Jpn. **64**, 4834 (1995).

[8] T. E. Mason, G. Aeppli, A. P. Ramirez, K. N. Clausen, C. Broholm, N. Stücheli, E. Bucher, and T. M. M. Palstra, Phys. Rev. Lett. **69**, 490 (1992).

[9] H. Kadowaki, T. Sato, H. Yoshizawa, T. Ekino, T. Takabatake, H. Fujii, L. P. Regnault, and Y. Ishikawa, J. Phys. Soc. Jpn. **63**, 2074 (1994); T. Sato, H. Kadowaki, H. Yashizawa, T. Ekino, T. Takabatake, H. Fujii, L. P. Regnault, and Y. Isikawa, J. Phys.: Condens. Matter **7**, 8009 (1995).

[10] S. Nishigori, H. Goshima, T. Suzuki, T. Fujita, G. Nakamoto, H. Tanaka, T. Takabatake, and H. Fujii, J. Phys. Soc. Jpn. **65**, 2614 (1996).

[11] M. Kyogaku, Y. Kitaoka, H. Nakamura, K. Asayama, T. Takabatake, F. Teshima, and H. Fujii, J. Phys. Soc. Jpn. **59**, 1728 (1990).

[12] K. Izawa, T. Suzuki, M. Kitamura, T. Fujita, T. Takabatake, G. Nakamoto, H. Fujii, and K. Maezawa, J. Phys. Soc. Jpn. **65**, 3119 (1996).

[13] A. Yanase and H. Harima, Prog. Theor. Phys. Suppl. **108**, 19 (1992).

[14] T. J. Hammond, G. A. Gehring, M. B. Suvasini, and W. M. Temmerman, Phys. Rev. B **51**, 2994 (1995).

[15] K. Ueda, H. Tsunetsugu, and M. Sigrist, Phys. Rev. Lett. **68**, 1030 (1992).

[16] H. Ikeda and K. Miyake, J. Phys. Soc. Jpn. **65**, 1769 (1996).

[17] S. Nohara, H. Namatame, A. Fujimori, and T. Takabatake, Phys. Rev. B **47**, 1754 (1993); Physica B **186-188**, 403 (1993).

[18] A. Slebarski, A. Jezierski, S. Mahl, M. Neumann, and G. Borstel, Phys. Rev. B **56**, 7245 (1997).

[19] J.-S. Kang, J. W. Allen, Z.-X. Shen, W. P. Ellis, J. J. Yeh, B. W. Lee, M. B. Maple, W. E. Spicer, and I. Lindau, J. Less-Common Met. **148**, 121 (1989).

[20] Note that the relative weights of spectral features from different valence states in the CIS or CFS spectra may not accurately reflect the valence in the case of strong hybridization.

[21] J. H. Scofield, J. Electron Spectrosc. Relat. Phenom. **8**, 129 (1976); J. J. Yeh and I. Lindau, At. Data Nucl. Data Tables **32**, 1 (1985).

[22] J. W. Allen, S.-J. Oh, O. Gunnarsson, K. Schönhammer, M. B. Maple, M. S. Torikachvili, and I. Lindau, Adv. Phys. **35**, 275 (1987).

[23] S. Hüfner and G. K. Wertheim, Phys. Lett. **51A**, 299 (1975); **51A**, 301 (1975).

[24] B. I. Min (unpublished).

[25] The off-resonance due to $4d \rightarrow 4f$ absorption corresponds to $h\nu \sim 115$ eV. However, our $h\nu = 115$ eV spectrum had a nonzero slope above E_F, probably due to the second-order light, which caused a distortion in the line shape of the difference curve. Since the valence-band spectrum with $h\nu = 115$ eV is essentially the same as that with $h\nu = 90$ eV except for the overall intensity, consistent with the dominant Ni $3d$ emission in this $h\nu$ range, the $h\nu = 90$ eV spectrum has been used in the subtraction. An appropriate correction has been made to account for the $h\nu$ dependence of the conduction electrons from $h\nu = 90$ eV to $h\nu = 115$ eV.

[26] Most of the surface Ce $4f$ emission is expected to be under the structure C in Ce $4f$ PSW.

[27] B. I. Min, H. J. F. Jansen, T. Oguchi, and A. J. Freeman, Phys. Rev. B **33**, 8005 (1986).

[28] O. Gunnarsson and K. Schönhammer, in *Handbook on the Physics and Chemistry of Rare Earths*, edited by K.A. Gschneidner, L. Eyring, and S. Hüfner (North-Holland, Amsterdam, 1987), Vol. 10, p. 103.

[29] J.-S. Kang, K. C. Kang, and B. I. Min, Physica B **230-232**, 497 (1997).

[30] E. Weschke, C. Laubschat, R. Ecker, A. Hohr, M. Domke, G. Kaindl, L. Severin, and B. Johansson, Phys. Rev. Lett. **69**, 1792 (1992).

[31] J. J. Joyce, A. J. Arko, J. Lawrence, P. C. Canfield, Z. Fisk, R. J. Bartlett, and J. D. Thompson, Phys. Rev. Lett. **68**, 236 (1992).

[32] A. B. Andrews, J. J. Joyce, A. J. Arko, J. D. Thompson, J. Tang, J. M. Lawrence, and J. C. Hemminger, Phys. Rev. B **51**, 3277 (1995).

[33] H. H. Hill, in *Plutonium 1970 and Other Actinides*, edited by W. N. Miner, special issue of Nucl. Metall. **17**, 2 (1970).

[34] J. M. Lawrence, A. J. Arko, J. J. Joyce, R. I. R. Blyth, R. J. Bartlett, P. C. Canfield, Z. Fisk, and P. S. Riseborough, Phys. Rev. B **47**, 15 460 (1993).

[35] C. G. Olson, P. J. Benning, M. Schmidt, D. W. Lynch, P. Canfield, and D. M. Wieliczka, Phys. Rev. Lett. **76**, 4265 (1996).

[36] There is uncertainty in the resonant strength of the $5d$ states with respect to that of the $4f$ states in Ce compounds. It is rather large in $CeBe_{13}$ (about 30–50 % in Ref. 34), but relatively small in CeSb ($\frac{1}{30}$ in Ref. 35).

[37] H.-D. Kim, O. Tjernberg, G. Chiaia, H. Kumigashra, T. Takahashi, L. Duo, O. Sakai, M. Kasaya, and I. Lindau, Phys. Rev. B **56**, 1620 (1997).

[38] N. E. Bickers, D. L. Cox, and J. W. Wilkins, Phys. Rev. Lett. **54**, 230 (1985).

[39] F. Gerken, A. S. Flodstrom, J. Barth, L. I. Johansson, and C. Kunz, Phys. Scr. **32**, 43 (1985).

[40] D. W. Lynch and R. D. Cowan, Phys. Rev. B **36**, 9228 (1987).

[41] O. Gunnarsson and T. C. Li, Phys. Rev. B **36**, 9488 (1987).

[42] L. Braicovich, C. Carbone, O. Gunnarsson, and G. L. Olcese, Phys. Rev. B **44**, 13 756 (1991).

[43] R. Haensel, P. Rabe, and B. Sonntag, Solid State Commun. **8**, 1845 (1970).

[44] V. A. Fomichev, T. M. Zimkina, S. A. Gribovskii, and I. I. Zhukova, Fiz. Tverd. Tela (Leningrad) **9**, 1163 (1967) [Sov. Phys. Solid State **9**, 1163 (1967)].